Joint Statistics of the Lagrangian Acceleration and Velocity in Fully Developed Turbulence

Alice M. Crawford, Nicolas Mordant,* and Eberhard Bodenschatz

Laboratory of Atomic and Solid State Physics, Clark Hall, Cornell University, Ithaca, New York, USA

(Received 13 August 2004; published 18 January 2005)

We report experimental results on the joint statistics of the Lagrangian acceleration and velocity in highly turbulent flows. The acceleration was measured up to a microscale Reynolds number $R_\lambda = 690$ using high speed silicon strip detectors from high energy physics. The acceleration variance was observed to be strongly dependent on the velocity, following a Heisenberg-Yaglom-like $u^{9/2}$ increase. However, the shape of the probability density functions of the acceleration component conditioned on the same component of the velocity when normalized by the acceleration variance was observed to be independent of velocity and to coincide with the unconditional probability density function of the acceleration components. This observation imposes a strong mathematical constraint on the possible functional form of the acceleration probability distribution function.

DOI: 10.1103/PhysRevLett.94.024501 PACS numbers: 47.27.Jv, 02.50.–r, 47.27.Gs

The classical theory of turbulence assumes a scale separation between the large scale at which energy is injected and the small scale at which it is dissipated. This would suggest the independence of small scale quantities like acceleration from large scale quantities like velocity. It has long been recognized that this independence of scales is only an approximation and our understanding of how small and large scale statistics may be related has gradually become increasingly sophisticated [1,2]. Experiment, simulations, theory, and modeling continue to interact to refine our understanding. Recently the study of acceleration statistics conditioned on the velocity has provided a new impetus for examining theory [2,3] and refining stochastic models [4–6].

Here we provide experimental evidence of the dependence of the Lagrangian acceleration on the velocity. The conditional acceleration variance varies strongly with the velocity which is not consistent with the assumption of local homogeneity. We discuss the dependence of the component acceleration variance on velocity in detail and then investigate the shape of the probability density function (PDF) of acceleration conditioned on velocity.

The flow and the acquisition system have been described in detail in a previous article [7]. The flow was of the von Kármán type: water was driven by two coaxial disks with blades and a rim, 20 cm in diameter, 33 cm apart, and enclosed in a cylindrical tank with a diameter of 48.3 cm. The disks were rotated at the same angular velocity but in opposite senses. Some parameters of the flow are shown in Table I. Note that the energy injection at large scales was anisotropic (the rms velocity being higher in the horizontal plane than along the axis of the disks) but that acceleration was much closer to isotropy, especially at the highest Reynolds number.

A schematic of the imaging system is displayed in Fig. 1. A 35 W pulsed laser illuminated the center of the flow. A $4.1 \times 4.1 \times 2.05$ mm^3 volume was imaged onto four silicon strip detectors (versus only two in the original design of [7]). Each one of these detectors was made of 512 strips (pixels) and recorded one component of the position. The flow was seeded with 25 μm polystyrene spheres with density 1.06 times that of water.

Since each detector recorded only one coordinate, it was necessary to match the four recordings to build a 3D track. The algorithm used to process the raw data has already been described in [7]. The magnitude of the intensity signal was used to match the x and z coordinates or the y and z coordinates for each pair of detectors. The last step consisted of matching the two recordings of the z component to get the full 3D trajectory. To compute the acceleration from the tracks, the position signal was convolved with a Gaussian kernel that both differentiated the position and filtered the noise [8].

Acceleration covariance conditional on velocity.— To check the dependence of acceleration on velocity, we first studied the tensor $\langle a_i a_j | u_k \rangle$. Because of the spatial reflection invariance of isotropic turbulence, the only nonzero components should be $\langle a_i^2 | u_k \rangle$. Although our flow was anisotropic at large scales, the acceleration was nearly isotropic and we found the $i \neq j$ terms to be zero within the experimental accuracy. The conditional variance of the acceleration components is presented in Fig. 2. One can see that for a given velocity component, the curves for the conditional variance of all three acceleration components are very similar. All three components vary strongly with the velocity, increasing more than 1 order of magnitude as the value of the velocity component goes from 0 to 4 times its rms value. It is interesting to note that the shape of the curves is dependent on the velocity component but not on the acceleration component. The ratio $\tilde{u}_t/\tilde{u}_z$ at $R_\lambda = 690$ is 1.78 (where $\tilde{u}_t$ and $\tilde{u}_z$ are horizontal and vertical rms velocities). If the abscissa axis were not normalized by the component rms velocity, the curves would split into two groups: those conditional on the vertical component and those conditional on the horizontal components. This is a result of the large scale

TABLE I. Parameters of the flow. f is the rotation frequency of the disks, $\tilde{u}_t = \langle u_x^2\rangle^{1/2} = \langle u_y^2\rangle^{1/2}$, $\tilde{u}_z = \langle u_z^2\rangle^{1/2}$, $\tilde{a}_t = \langle a_x^2\rangle^{1/2} = \langle a_y^2\rangle^{1/2}$, $\tilde{a}_z = \langle a_z^2\rangle^{1/2}$, ϵ is the dissipation rate (the uncertainty is about 15% [7]), $\tau_\eta = \sqrt{\nu/\epsilon}$ is the Kolmogorov time ($\nu = 0.989 \times 10^{-6}$ m^2 s^{-1} is the kinematic viscosity), $\eta = (\nu^3/\epsilon)^{1/4}$ is the Kolmogorov length, R_λ is the Taylor scale Reynolds number, and δt is the sampling interval.

f	$\tilde{u}_t$	$\tilde{u}_z$	$\tilde{a}_t$	$\tilde{a}_z$	ϵ	τ_η	η	R_λ	δt
Hz	ms^{-1}	ms^{-1}	ms^{-2}	ms^{-2}	m^{2}s^{-3}	ms	μm		μs
0.6	0.082	0.049	1.52	1.41	5.77×10^{-3}	13.1	114	285	74.9
1	0.245	0.143	18.0	16.7	0.143	2.63	51	485	25.9
3.5	0.50	0.28	87.0	84.6	1.14	0.929	30	690	14.3

velocity being anisotropic while the small scale acceleration is nearly isotropic.

For isotropic homogeneous turbulence, the conditional acceleration covariance tensor can be rewritten as

$$\langle a_i a_j|\mathbf{u}\rangle = \sigma_a^2[f(u) - g(u)]\frac{u_i u_j}{u^2} + \sigma_a^2 g(u)\delta_{ij}, \qquad (1)$$

where $\sigma_a^2 = \frac{1}{3}\langle \mathbf{a}^2\rangle$; f and g are normalized conditional variances of acceleration components parallel and perpendicular to the velocity vector, respectively. f and g depend only on the velocity magnitude u. We cannot check directly the validity of this expression as the convergence requires data sets larger by orders of magnitude. What is within our reach, however, is to study $\langle a_i a_j|u\rangle$, the acceleration covariance tensor conditioned on the magnitude of the velocity and f and g.

Figure 3 displays $\langle a_i a_j|u\rangle$ for all combinations of (i, j) at $R_\lambda = 690$. One can see that for $i \neq j$, the covariance fluctuates about zero and takes on much smaller values than the diagonal terms. The off-diagonal terms of the covariance tensor can be considered to be zero within the experimental accuracy. For the case $i = j$, the conditional variance increases strongly with u and the curves for all three components collapse. The use of the velocity magnitude seems to have removed the influence of the large scale anisotropy. The conditional acceleration varies by a factor of 20 as the velocity magnitude goes from 0 to $5u_{\rm rms}$.

The Heisenberg-Yaglom scaling of the full acceleration variance is $\langle a^2\rangle = a_0\epsilon^{3/2}\nu^{-1/2}$ [9] but can also be rewritten as $\langle a^2\rangle \propto \sigma_u^{9/2}L^{-3/2}\nu^{-1/2}$ as $\epsilon \propto \sigma_u^3/L$ (σ_u is the velocity component rms value, L is the flow integral scale). As pointed out by Aringazin and Mazhitov [3], this suggests a natural scaling for the conditional acceleration variance

$$\langle a^2|u\rangle \propto u^{9/2}. \qquad (2)$$

Noting that $\langle a^2|u = 0\rangle$ is strictly positive, we fitted the experimental normalized conditional acceleration variance

$$\langle a^2|u\rangle/\sigma_a^2 = \alpha + \beta(u/\sigma_u)^{9/2} \qquad (3)$$

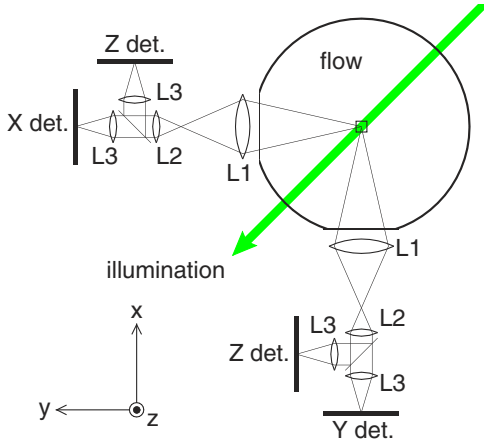

FIG. 1 (color online). Top view of the setup of the imaging system. A small measurement volume of size $4.1 \times 4.1 \times 2.05$ mm^3 at the center of the flow was illuminated by a 35 W pulsed laser. This volume was then imaged at 45° scattering angle in the midplane of the cylindrical tank, so as to record the three coordinates of the particle motion in the flow. The characteristics of the optics were identical to those in [7]. The rotation axis of the disks was along the z direction.

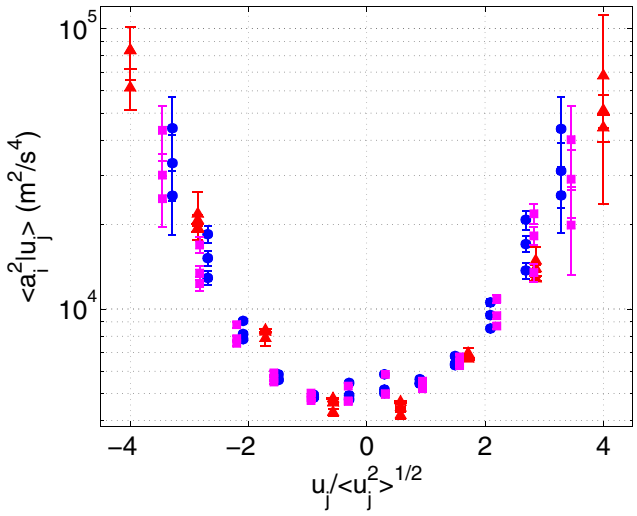

FIG. 2 (color online). Conditional acceleration component variance $\langle a_i^2|u_j\rangle$ at $R_\lambda = 690$. The velocity components have been normalized by their variance. Circles: $\langle a_i^2|u_y\rangle$, squares: $\langle a_i^2|u_x\rangle$, and triangles: $\langle a_i^2|u_z\rangle$.

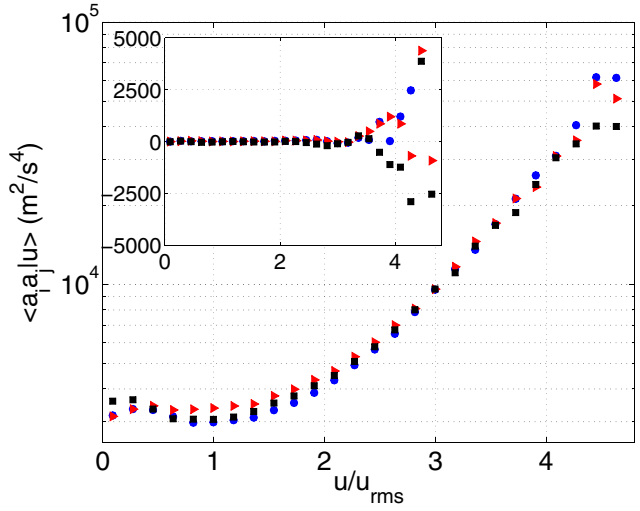

FIG. 3 (color online). Acceleration covariance conditioned on velocity magnitude $\langle a_i a_j | u \rangle$ at $R_\lambda = 690$. The main window contains the diagonal terms ($i = j$) and the insert contains the off-diagonal terms ($i \neq j$). $u_{\rm rms} = \sqrt{\frac{1}{3}(2\tilde{u}_t^2 + \tilde{u}_z^2)} = 0.43$ m/s.

as shown in Fig. 4. The fit gives $\alpha = 2.6$, 2.06, 2.10 and $\beta = 0.012$, 0.029, 0.032 for $R_\lambda = 285$, 485, and 670, respectively. The agreement between the data and the fit is striking. At the smallest Reynolds number, the acceleration variance is increasing much less. The curves corresponding to the two highest Reynolds numbers almost superimpose, suggesting a convergence at high Reynolds number. Note that a similar fit based on the multifractal scaling proposed by Biferale *et al.* [2], $\langle a^2 | u \rangle \propto u^{4.57}$ is not distinguishable within the precision of the experiment. Sawford *et al.* [5] suggested a u^6 scaling and proposed an argument based on vorticity tubes to explain it. The $u^{9/2}$ scaling, however, is more consistent with the data.

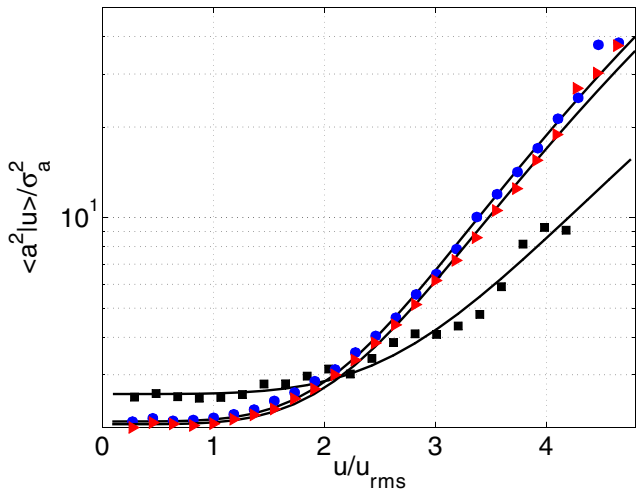

FIG. 4 (color online). Normalized conditional acceleration variance $\langle a^2 | u \rangle / \sigma_a^2$ for $R_\lambda = 690$, 485, 285, circles, triangles, and squares, respectively. Solid lines are the fit (3).

We now project the acceleration onto another set of axes. It is split into the component parallel to velocity and two components perpendicular both to each other and to the velocity. Figure 5 shows the conditional average and variance of these components. As shown in the insert, the average acceleration conditioned on the velocity magnitude remains less than 5% of $\sqrt{\langle a_i^2 | u \rangle}$ and is zero within the experimental accuracy. The main window displays the parallel $[f(u)]$ and perpendicular $[g(u)]$ acceleration variances. They are seen to be slightly different, the parallel one being smaller than the perpendicular ones. The two perpendicular variances superimpose within the error. In this figure we also compare our data with direct numerical simulations (DNS) of homogeneous and isotropic turbulence at $R_\lambda = 420$ [5]. The experimental and DNS results are qualitatively similar; the DNS curves increase faster than the experimental one. The dependence of the experimental curves on the Reynolds number (Fig. 4) is stronger than reported from DNS [5]

Joint distribution of acceleration and velocity components.—So far, we have only considered the second moment of the acceleration conditioned on the velocity. We have sufficient statistics to investigate the shape of the PDF of an acceleration component conditioned on the value of the same component of velocity: $P(a_i | u_i)$. We already observed that the width of the PDF increases with u_i. To see a possible change in the shape, we plot in Fig. 6 the conditional PDFs normalized by the conditional variance so that for any given value of u_y the variance of the PDF is unity. Within the uncertainty of the measurement, no change of shape can be observed. These conditional PDFs are also compared to the unconditional PDF of the

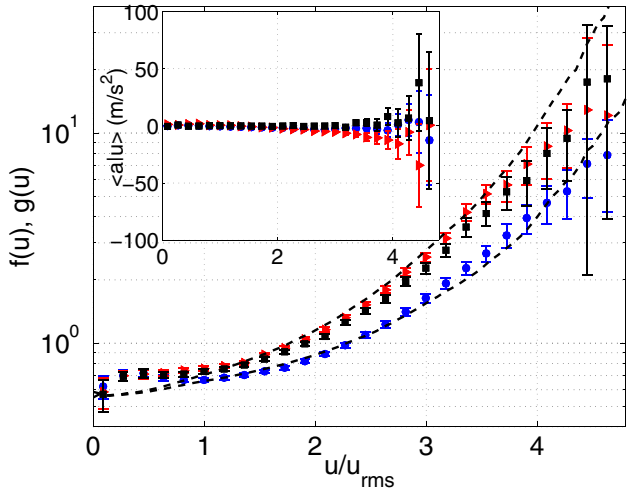

FIG. 5 (color online). Acceleration variance conditioned on velocity magnitude at $R_\lambda = 690$. Circles: acceleration parallel to the velocity vector $[f(u)]$; squares and triangles: acceleration perpendicular to the velocity $[g(u)]$. Dashed lines: f and g from DNS at $R_\lambda = 420$ [5]. The insert shows the mean acceleration conditioned on u (same symbols).

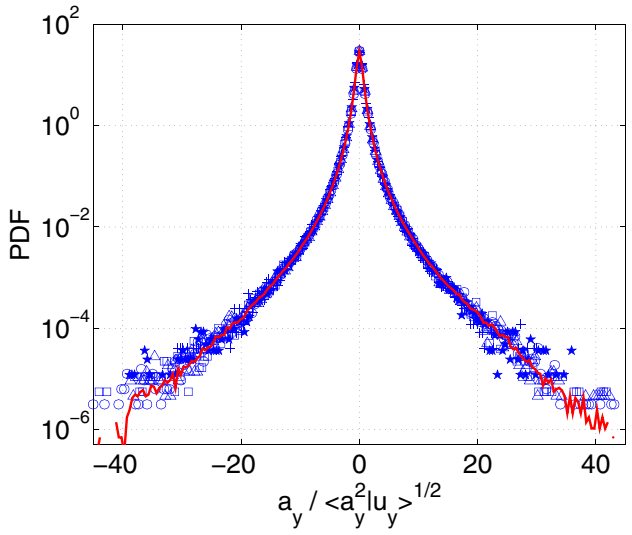

FIG. 6 (color online). PDFs of acceleration conditioned on velocity at $R_\lambda = 690$. Symbols show normalized conditional acceleration component PDFs for various values of the velocity $\circ u_y = 0$, $\triangle u_y = 0.5\tilde{u}_t$, $\square u_z = \tilde{u}_t$, $\star u_y = 1.5\tilde{u}_t$, $+u_y = 2\tilde{u}_t$. The solid line shows the normalized unconditional acceleration component PDF $P(a_y/\langle a_y^2\rangle^{1/2})$.

acceleration component $P(a)$. The unconditional PDF is superimposed on all the other curves. It seems that the dependence of acceleration on the velocity is totally taken into account by the variance. This imposes constraints on the functional form of the PDF of acceleration. Let us call this functional form $\mathcal{P}$. By definition,

$$P(a_i) = \int_{-\infty}^{+\infty} P(a_i|u_i)P(u_i)du_i. \quad (4)$$

If we assume that the functional form of the conditional PDF is the same as that of the unconditional one, then $\mathcal{P}$ must obey

$$\mathcal{P}(a) = \int_{-\infty}^{+\infty} \frac{\sigma_a}{\sigma_{a|u}} \mathcal{P}\left(\frac{\sigma_a}{\sigma_{a|u}} a\right) \frac{1}{\sqrt{2\pi\sigma_u^2}} e^{(-u^2/2\sigma_u^2)} du, \quad (5)$$

where $\sigma_{a|u} = \sqrt{\langle a^2|u\rangle}$, and σ_a and σ_u are the acceleration and velocity component rms values. We assume that the PDF of the velocity components is Gaussian which was verified experimentally [10]. This equation restricts considerably the possible functional form of $\mathcal{P}$. α-stable distributions are possible candidates [11].

Our unique experimental setup allowed us to study complex quantities such as the statistics of the acceleration conditional on the velocity at sufficiently high Reynolds numbers, where the universal properties may be expected. We observed a strong dependence of acceleration on velocity which is at odds with the assumption of local homogeneity. We observed that the conditional acceleration variance strongly increases with velocity following a $u^{9/2}$ scaling inspired by the Heisenberg-Yaglom scaling of the full acceleration variance. This scaling is also in agreement with the multifractal scaling prediction proposed by Biferale *et al.* [2]. The dependence of acceleration on velocity appears to be contained in the conditional variance. The conditional PDF of acceleration also collapses onto the unconditional one. This observation imposes a constraint on the possible functional form of the latter PDF restricting considerably the class of admissible distributions.

We are very grateful to Professor B. L. Sawford and P. K. Yeung for providing us with the DNS data from [5]. This work was supported by NSF Grant No. 9988755.

*Present address: Laboratoire de Physique Statistique, Ecole Normale Supérieure, Paris, France.
Email: nmordant@ens.fr.

[1] U. Frisch, *Turbulence* (Cambridge University Press, Cambridge, England, 1995).
[2] L. Biferale, G. Boffetta, A. Celani, B. J. Devenish, A. Lanotte, and F. Toschi, Phys. Rev. Lett. **93**, 064502 (2004).
[3] A. K. Aringazin and M. I. Mazhitov, cond-mat/0408018.
[4] B. L. Sawford, Phys. Fluids A **3**, 1577 (1991).
[5] B. L. Sawford, P. K. Yeung, M. S. Borgas, P. Vedula, A. La Porta, A. M. Crawford, and E. Bodenschatz, Phys. Fluids **15**, 3478 (2003).
[6] A. M. Reynolds, Phys. Rev. Lett. **91**, 084503 (2003).
[7] G. A. Voth, A. L. Porta, A. M. Crawford, J. Alexander, and E. Bodenschatz, J. Fluid Mech. **469**, 121 (2002).
[8] A. M. Crawford, Ph.D. thesis, Cornell University, 2004.
[9] A. La Porta, G. A. Voth, A. M. Crawford, J. Alexander, and E. Bodenschatz, Nature (London) **409**, 1017 (2001).
[10] N. Mordant, P. Metz, O. Michel, and J.-F. Pinton, Phys. Rev. Lett. **87**, 214501 (2001).
[11] P. Chainais (private communication).